Nuclear structure in ^{95,97}Ru nuclei

P. Chowdhury,* B. A. Brown,† U. Garg,‡ R. D. McKeown,§ T. P. Sjoreen,** and D. B. Fossan
Department of Physics, State University of New York, Stony Brook, New York 11794
(Received 1 July 1985)

The high-spin level structures of the nuclei ^{95,97}Ru have been studied via the ^{92}Mo(^{6}Li,p2n)^{95}Ru and ^{93}Nb(^{7}Li,3n)^{97}Ru reactions, using γ-γ coincidence, γ-$W(\theta)$, and pulsed-beam-γ measurements. Shell-model calculations of energy levels and $B(E2)$ values for ^{95}Ru have been performed and compared with the experimentally observed levels and the measured $\frac{21}{2}^+$ and $\frac{17}{2}^+$ lifetimes. A collective $\Delta J=2$ band has been identified with the $1h_{11/2}$ neutron state in ^{97}Ru, and discussed in the context of the general nature of collectivity in nuclei outside the $N=50$ closed shell. No $\Delta J=1$ band associated with the $1g_{9/2}$ neutron-hole intruder state was found in either of the $N=51,53$ Ru nuclei, as observed previously for the $1g_{9/2}$ proton-hole intruder states in the $Z=51$ Sb and $Z=53$ I nuclei.

I. INTRODUCTION

The level structures of Ru nuclei immediately outside the $N=50$ closed shell provide information on both quasiparticle and collective degrees of freedom in this region. From a viewpoint of the shell model, levels in $N=50$ nuclei are reasonably well described using effective interactions within a limited configuration space, with the protons occupying the $2p_{1/2}$ and $1g_{9/2}$ orbitals above an inert $_{38}Sr_{50}$ core. The low-lying states of the nucleus $^{94}Ru_{50}$, in particular, conform rather well to the $(\pi g_{9/2})^n$ seniority-two structure of an even-even $N=50$ nucleus.[1,2] Consequently, the high-spin states of the ^{95,97}Ru nuclei, with one and three neutrons, respectively, outside the $N=50$ closed shell, are well suited for the study of n-p effective interactions involving the proton orbitals below $Z=50$ and the neutron orbitals outside $N=50$. On the other hand, odd-mass Ru nuclei with $N\geq 55$ have been found to exhibit collective behavior in the form of systematic $\Delta J=2$ bands built on $\frac{11}{2}^-$ states.[3] These have been interpreted as "decoupled" bands built on $1h_{11/2}$ quasineutron states, where the intraband transition energies follow the ground-state-band spacings of the even-even $(A-1)$ core. The level structures of ^{95,97}Ru, therefore, should allow a mapping of these collective effects in Ru nuclei, from regions of sizable deformation near the middle of the neutron shell ($50\leq N\leq 82$) towards the spherical $N=50$ shell closure.

In addition, the nuclei ^{95,97}Ru are good candidates for exploring for the coexistence of the strong collectivity often associated with intruder hole states from across closed shells ($N=50$). Nuclei in the vicinity of other closed shells have been found to exhibit such characteristics for intruder states. In the region above the $Z=50$ closed shell, in addition to decoupled $\Delta J=2$ bands exhibiting modest collectivity, systematic $\Delta J=1$ bands have been observed, built on $1g_{9/2}$ proton-hole states, in Sb ($Z=51$) (Ref. 4), I ($Z=53$) (Refs. 5 and 6), and Cs ($Z=55$) (Ref. 7) nuclei. The surprisingly low excitation energies of the $\frac{9}{2}^+$ bandheads, which have minima near the middle of the 50—82 neutron shell, have been primarily attributed to collective effects. The best environment for a search for analogous band structures in the $N>50$ region, wherein the bandhead would be a $1g_{9/2}$ neutron hole, is provided by the nuclei ^{95,97}Ru, with $N=51$ and 53, respectively. This is because these Ru ($Z=44$) isotopes occur in the middle of the 38—50 proton subshell, where collective effects within the subshell are expected to be maximized. Consequently the $(\nu g_{9/2})^{-1}$ states and the associated band structures might be expected to lie at low excitation energies in these nuclei, and be easily populated via heavy-ion fusion-evaporation reactions.

Previous studies[3] of the high-spin states of these nuclei utilized (α,xn) reactions. The present work has been carried out with ^{6,7}Li beams in order to increase the total angular momentum brought into the compound system, and thus populate considerably higher spin states in the residual nuclei. Preliminary results of this work have been reported earlier.[8,9] Subsequent to this work singles measurements of excitation functions, angular distributions, and lifetimes in ^{97}Ru have been reported,[10] using (^{12}C,3n) reactions.

II. EXPERIMENTAL PROCEDURE

The nuclei ^{95,97}Ru were studied using the reactions ^{92}Mo(^{6}Li,p2n)^{95}Ru and ^{93}Nb(^{7}Li,3n)^{97}Ru. The ^{6,7}Li beams were obtained from the Stony Brook FN tandem Van de Graaff accelerator, and were incident on self-supporting, isotopically enriched ^{92}Mo and ^{93}Nb targets, with thicknesses of 10 and 5 mg/cm^2, respectively. Excitation function measurements were carried out with beam energies ranging from 28 to 34 MeV. On the basis of these measurements, bombarding energies of 34 MeV ^{6}Li and 30 MeV ^{7}Li were chosen to optimize the relative yields of the respective residual nuclei.

The deexcitation γ rays of the ^{95,97}Ru nuclei were detected with coaxial Ge(Li) detectors ($\sim$10% efficiency), having energy resolutions of 2.0—2.2 keV FWHM at 1.33 MeV. In order to identify the γ-ray cascades in the vari-

ous residual nuclei, γ-γ coincidence measurements were performed. Information on γ-ray multipolarities and intensities (I_γ) was obtained from γ-ray angular distribution measurements, recorded in singles mode at four angles between 90° and 150° to the beam direction. The extracted photopeak intensities were fitted to

$$W(\theta)=I_\gamma[1+A_2P_2(\cos\theta)+A_4P_4(\cos\theta)]\ ,$$

where P_2,P_4 are Legendre polynomials. The intensity and anisotropy information was used to make spin assignments, assuming a high degree of alignment (low-m substate population) of the high-spin states of the residual nuclei, and their subsequent decay via stretched ($J\rightarrow J-L$) transitions, involving primarily the yrast states. These assumptions have been found to be valid for the γ-decay modes for a large number of fusion-evaporation reactions.

For the ^{95}Ru nucleus, delayed γ-coincidence and lifetime measurements were performed to search for and study isomeric states and their decay modes. The lifetimes of the $\frac{21}{2}^+$ and $\frac{17}{2}^+$ states were measured using ^{6}Li beam pulses with a repetition period of 250 ns and a pulse width of $\sim$2 ns. The pulsed beam measurements also furnished lifetime limits for the various nuclear levels, which were used to rule out the existence of high multipolarities in decay transitions.

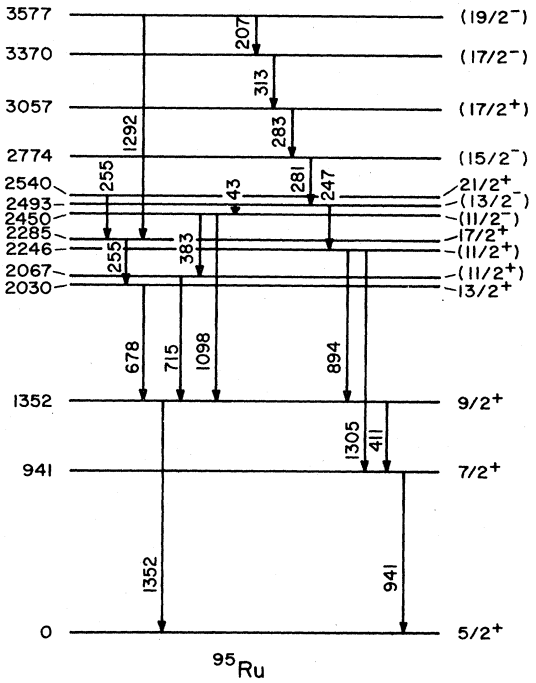

FIG. 1. Level scheme for ^{95}Ru (from present work). All energies are in keV.

III. EXPERIMENTAL RESULTS

A. ^{95}Ru

The level scheme of ^{95}Ru deduced from the present work is shown in Fig. 1. The results of the γ-ray angular distribution measurements from the ^{92}Mo(^{6}Li,2n)^{95}Ru reaction are presented in Table I. The strong cascade of γ rays, with energies (from the bottom) of 1352, 678, and 255 keV, was confirmed, as previously observed by Lederer *et al.*[3] via the (α, 2n) reaction. However, the 255-keV γ ray is found to be in coincidence with itself. Thus two

TABLE I. Angular distribution results for ^{95}Ru.

E_γ[a] (keV)	I_γ[b]	A_2	A_4[c]	Assignment
207	4	−0.26±0.03	−0.07±0.04	$(\frac{19}{2}^-)\rightarrow(\frac{17}{2}^-)$
247	6	−0.24±0.06		$(\frac{13}{2}^-)\rightarrow(\frac{11}{2}^+)$
255[d]	59	0.31±0.01	−0.11±0.02	$\frac{21}{2}^+\rightarrow\frac{17}{2}^+$, $\frac{17}{2}^+\rightarrow\frac{13}{2}^+$
281	8	−0.15±0.05		$(\frac{15}{2}^-)\rightarrow(\frac{13}{2}^-)$
283	3	−0.29±0.11		$(\frac{17}{2}^+)\rightarrow(\frac{15}{2}^-)$
313	5	−0.21±0.05	−0.06±0.06	$(\frac{17}{2}^-)\rightarrow(\frac{17}{2}^+)$
411	3	−0.26±0.06		$\frac{9}{2}^+\rightarrow\frac{7}{2}^+$
678	62	0.28±0.05	−0.04±0.06	$\frac{13}{2}^+\rightarrow\frac{9}{2}^+$
715	5	0.18±0.06		$(\frac{11}{2}^+)\rightarrow\frac{9}{2}^+$
894	8	0.01±0.04		$(\frac{11}{2}^+)\rightarrow\frac{9}{2}^+$
941	26	0.13±0.02	0.11±0.03	$\frac{7}{2}^+\rightarrow\frac{5}{2}^+$
1292	12	0.27±0.05		$(\frac{19}{2}^-)\rightarrow\frac{17}{2}^+$
1305	4	0.20±0.13		$(\frac{11}{2}^+)\rightarrow\frac{7}{2}^+$
1352	100	0.32±0.02	−0.08±0.02	$\frac{9}{2}^+\rightarrow\frac{5}{2}^+$

[a]Energies are given to the nearest keV.
[b]All intensities have been normalized to the 1352-keV line, and are accurate to ±10% for the stronger γ rays. For $I_\gamma<10$, an absolute ΔI_γ of ±1 is more appropriate.
[c]Wherever not quoted, the values were consistent with O.O.
[d]Doublet in this nucleus.

255-keV γ rays have been placed in cascade in the level scheme. On the basis of the angular distribution data, spin assignments of $\frac{9}{2}^+$, $\frac{13}{2}^+$, $\frac{17}{2}^+$, and $\frac{21}{2}^+$ are made for the 1352- 2030-, 2285-, and 2450-keV levels, with a ground-state spin of $\frac{5}{2}^+$. Weaker γ rays were observed and have been included in the level scheme. Levels up to a maximum excitation energy of 3577 keV were established. Spin assignments in parentheses are tentative.

Both the 255-keV γ rays were found to be delayed. In the previous lifetime analysis of Lederer *et al.*,[3] however, a single 255-keV γ ray had been assumed to be present, leading to a mean lifetime of 8.3 ± 1.0 ns for the $\frac{17}{2}^+$ level. In the present work, the lifetimes of the $\frac{21}{2}^+$ and $\frac{17}{2}^+$ levels have been measured, taking into account the presence of two 255-keV transitions in cascade. The time differential spectrum of the 255-keV doublet was fitted to the function

$$f(t)=A_0+(A_1/\tau_1)e^{-t/\tau_1}+(A_2/\tau_2)e^{-t/\tau_2}$$
$$+[A_1/(\tau_1-\tau_2)](e^{-t/\tau_1}-e^{-t/\tau_2}),$$

where τ_1 and τ_2 are the mean lifetimes of the $\frac{21}{2}^+$ and $\frac{17}{2}^+$ levels, respectively, A_1 is the feeding intensity of the $\frac{21}{2}^+$ level, A_2 is the side-feeding intensity of the $\frac{17}{2}^+$ level, and A_0 is a normalization constant. The data are

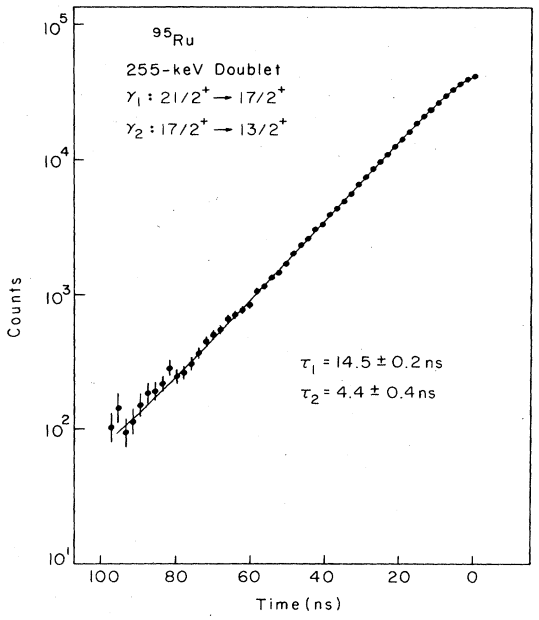

FIG. 2. Time differential spectrum of the 255-keV γ-ray doublet comprising the $\frac{21}{2}^+ \rightarrow \frac{17}{2}^+$ and $\frac{17}{2}^+ \rightarrow \frac{13}{2}^+$ transitions in ^{95}Ru. The solid line is a two-lifetime least squares fit to the data (see the text).

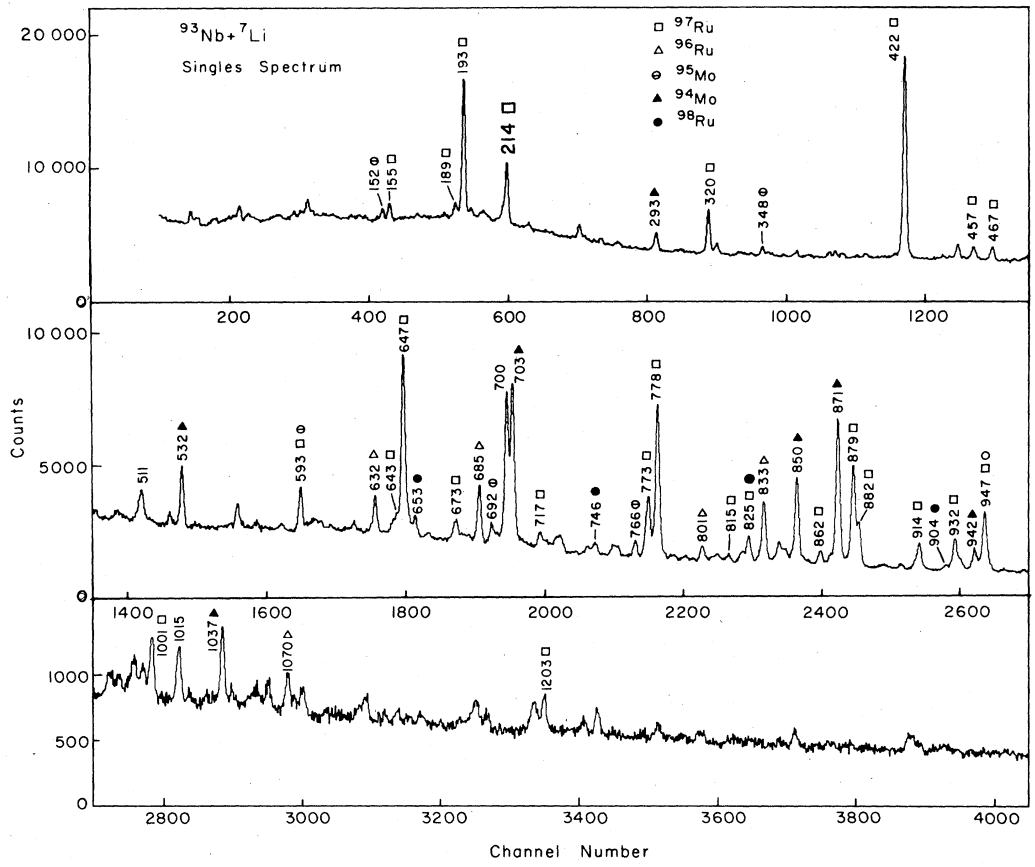

FIG. 3. Singles γ-ray spectrum for the ^{93}Nb+^{7}Li reaction. Energies for the γ rays of various evaporation channels are marked in keV.

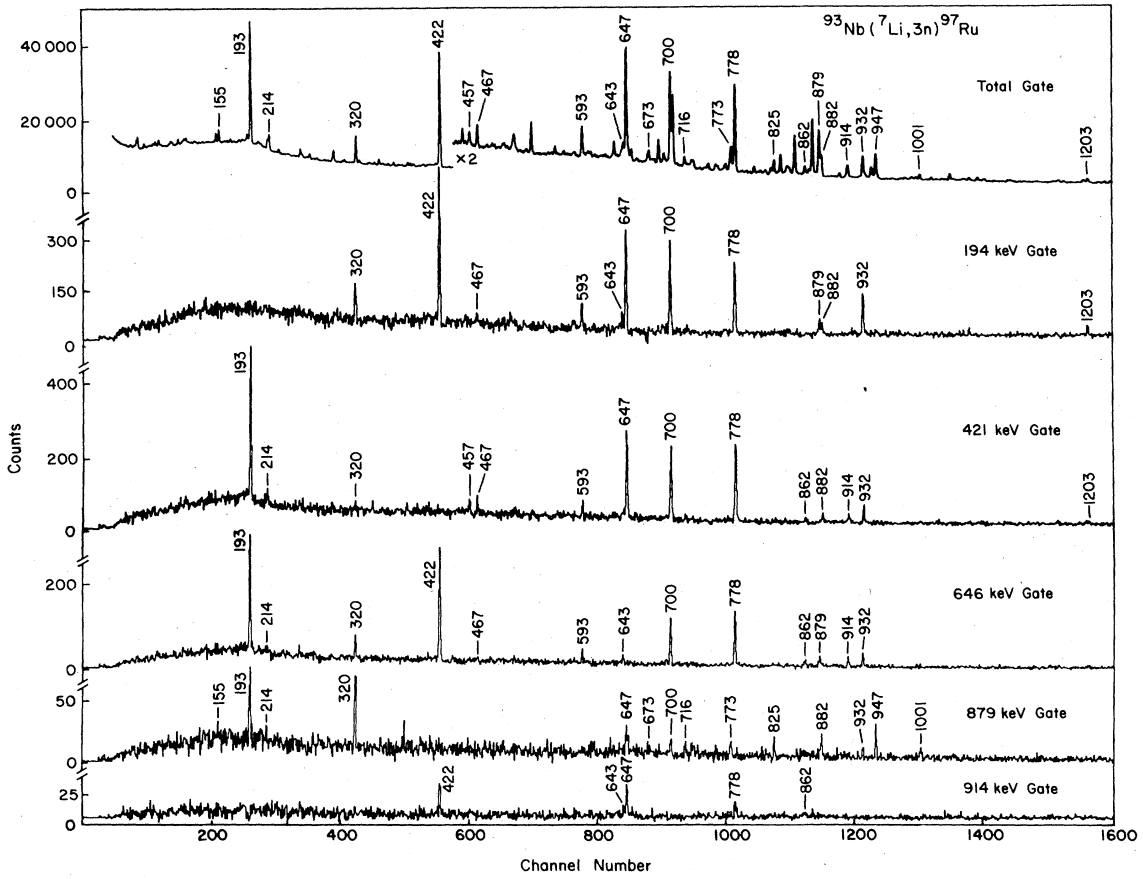

FIG. 4. Representative γ-γ coincidence spectra for the ^{97}Ru nucleus.

shown in Fig. 2, along with the best fit (minimum χ^2) using the above expression. A single-lifetime fit to the data resulted in significantly higher χ^2 values (a factor of ~ 5) than the two-lifetime fit. The analysis yields a mean lifetime τ of 14.5±0.2 ns for the $\frac{21}{2}^+$ level and 4.4±0.4 ns for the $\frac{17}{2}^+$ level.

B. ^{97}Ru

The high-spin level structure of ^{97}Ru was studied via a ^{93}Nb(^{7}Li,3n) reaction using a 30 MeV ^{7}Li beam. A singles γ-ray spectrum is shown in Fig. 3, where the cross section for three-neutron evaporation is seen to be dominant. Representative γ-γ spectra for the ^{97}Ru nucleus are shown in Fig. 4. The angular distribution results are presented in Table II, and the level scheme of ^{97}Ru from the present work is shown in Fig. 5.

States up to a maximum excitation energy of 4731 keV and spin of $\frac{29}{2}^+$ were observed. The strongest cascade in the γ decay of the nucleus is shown on the left in the level scheme. The γ rays observed in this cascade below the 2739-keV level, and the J^π assignments for the associated levels, are in agreement with earlier (α,n) work by Lederer *et al.*[3] Spin assignments for the higher levels are based on the γ-ray angular distributions, assuming a dominance of stretched transitions. The large positive A_2 and small negative A_4 coefficients for the 914- and 862-keV γ rays identify these as stretched $J \rightarrow J-2$ quadrupole transitions, leading to J^π assignments of $\frac{19}{2}^+$ and $\frac{23}{2}^+$ for the 2759- and 3621-keV levels, respectively. Precise angular distribution coefficients could not be obtained for the

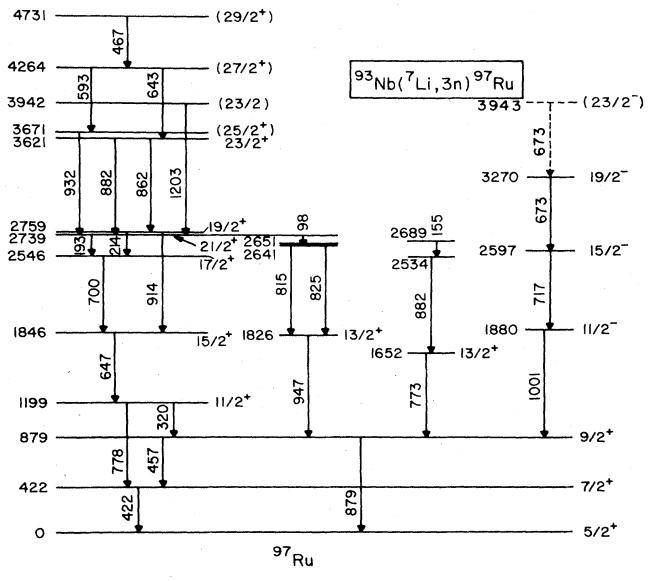

FIG. 5. Level scheme for ^{97}Ru (from the present work). All energies are in keV.

TABLE II. Angular distribution results for ^{97}Ru.

E_γ[a] (keV)	I_γ[b]	A_2	A_4[c]	Assignment
155.1	3	−0.18±0.04	0.13±0.06	
193.4	40	0.03±0.02	−0.08±0.03	$\frac{21}{2}^+ \rightarrow \frac{17}{2}^+$
214.0[d]	6	0.09±0.19		$\frac{19}{2}^+ \rightarrow \frac{17}{2}^+$
319.9	15	−0.27±0.02		$\frac{11}{2}^+ \rightarrow \frac{9}{2}^+$
421.5	100	−0.07±0.02	0.05±0.02	$\frac{7}{2}^+ \rightarrow \frac{5}{2}^+$
457.2	9	−0.18±0.04		$\frac{9}{2}^+ \rightarrow \frac{7}{2}^+$
466.8	8	−0.15±0.04		$(\frac{29}{2}^+) \rightarrow (\frac{27}{2}^+)$
593.3[d]	14	−0.18±0.03	0.05±0.04	$(\frac{27}{2}^+) \rightarrow (\frac{25}{2}^+)$
646.5	89	0.29±0.02	−0.01±0.03	$\frac{15}{2}^+ \rightarrow \frac{11}{2}^+$
673.3[e]	13	0.26±0.04	−0.07±0.05	$\frac{19}{2}^- \rightarrow \frac{15}{2}^-$, $(\frac{23}{2}^-) \rightarrow \frac{19}{2}^-$
699.9	68	−0.21±0.02		$\frac{17}{2}^+ \rightarrow \frac{15}{2}^+$
716.9	8	0.25±0.04	−0.11±0.06	$\frac{15}{2}^- \rightarrow \frac{11}{2}^-$
772.7	44	0.03±0.02	−0.03±0.03	$\frac{13}{2}^+ \rightarrow \frac{9}{2}^+$
777.6	89	0.25±0.02	−0.03±0.03	$\frac{11}{2}^+ \rightarrow \frac{7}{2}^+$
814.5	5	0.24±0.09	0.25±0.11	$\rightarrow \frac{13}{2}^+$
824.8[d]	13	−0.01±0.04	0.11±0.05	$\rightarrow \frac{13}{2}^+$
862.1	9	0.25±0.04	−0.01±0.06	$\frac{23}{2}^+ \rightarrow \frac{19}{2}^+$
879.2	71	0.24±0.02	−0.04±0.03	$\frac{9}{2}^+ \rightarrow \frac{5}{2}^+$
882.3[e]	19	0.17±0.03	0.19±0.04	$\frac{23}{2}^+ \rightarrow \frac{21}{2}^+$, $\rightarrow \frac{13}{2}^+$
913.7	21	0.28±0.03	−0.01±0.04	$\frac{19}{2}^+ \rightarrow \frac{15}{2}^+$
932.0	22	0.33±0.04	0.02±0.06	$(\frac{25}{2}^+) \rightarrow \frac{21}{2}^+$
947.5[d]	44	0.16±0.02	0.03±0.03	$\frac{13}{2}^+ \rightarrow \frac{9}{2}^+$
1000.6	8	−0.10±0.05	0.18±0.07	$\frac{11}{2}^- \rightarrow \frac{9}{2}^+$
1202.9	5	−0.23±0.07		$(\frac{23}{2}) \rightarrow \frac{21}{2}^+$

[a]Energies are within 0.3 keV.
[b]All intensities have been normalized to the 421.5-keV line, and are accurate to ±10% for the stronger γ rays. For $I_\gamma < 10$; an absolute ΔI_γ of ±1 is more appropriate.
[c]Wherever not quoted, the values were consistent with O.O.
[d]Contaminant γ ray for competing channel present.
[e]Doublet in this nucleus.

643-keV γ ray due to the proximity of the strong 647-keV transition. However, a ratio of the intensities of 90° and 150° angles suggests a quadrupole nature for the 643-keV transition, while the A_k coefficients for the 467-keV γ ray are consistent with those of a stretched $J \rightarrow J-1$ dipole transition. This leads to tentative assignments of $(\frac{27}{2}^+)$ and $(\frac{29}{2}^+)$ for 4264- and 4731-keV levels, respectively. The angular distributions of the 593- and 932-keV transitions populating and depopulating the 3671-keV level, respectively, suggest a $(\frac{25}{2}^+)$ assignment for that level. The levels and spin assignments up to the 4264-keV $\frac{27}{2}^+$ level in this cascade agree with subsequent (^{12}C,3n) results of Bucurescu *et al.*,[10] who have shown a partial level scheme of ^{97}Ru taken from unpublished (α,2n) measurements of Hseuh *et al.*[11]

A weak $\Delta J = 2$ band was observed, built on an $\frac{11}{2}^-$ state at 1880 keV. A J^π assignment of $\frac{11}{2}^-$ for the 1880-keV level is consistent with the population of this state via $L = 5$ transfer strength in the ^{96}Ru(d,p)^{97}Ru reaction.[12,13] The $\Delta J = 2$ band consists of γ rays with energies (from the bottom) of 717, 673, and (673) keV. Both the coincidence and intensity information suggest a 673-keV doublet in cascade above the 717-keV γ ray. The angular distributions of the 717- and 673-keV γ rays are consistent with stretched $E2$ character. Thus, spin assignments of $\frac{15}{2}^-$, $\frac{19}{2}^-$, and $(\frac{23}{2}^-)$ are proposed for the 2597-, 3270-, and 3943-keV levels, respectively. An additional interesting question is whether the 3942-keV level depopulated by a 1203-keV γ ray is the same as the 3943-keV level, $(\frac{23}{2}^-)$ state of the negative parity band. The angular distribution of the 1203-keV γ ray suggests a spin of $\frac{23}{2}$ for the 3942-keV level, and the energy match is within the limits of experimental error. If the $(\frac{23}{2}^-)$ state is indeed connected to the $\frac{21}{2}^+$ state via the 1203-keV transition, the implied lack of purity of the $\Delta J = 2$ band would indicate a rather weak collectivity in this nucleus. This band, which has not been identified in the (α,n) and (^{12}C,3n) studies, will be discussed in the context of similar bands observed in heavier odd-A Ru nuclei.

Several other weaker γ rays were observed and have been included in the level scheme. These document additional levels in ^{97}Ru. Our placement of the 773-882-keV

cascade feeding the 879-keV level disagrees with the scheme shown in Ref. 10 obtained from Hseuh *et al.*,[11] as this cascade is not found to be in coincidence with the 947-keV transition in the present work. Tentative spin-parity assignments have been denoted with parentheses in our level scheme.

IV. DISCUSSION

A. ^{95}Ru

It is expected that the excited level structure of the $N=51$ nucleus ^{95}Ru will have a simple shell-model description, owing to the good $N=50$ shell closure and the partial proton shell closure at $Z=38$. In order to make a reasonable comparison, theoretical energy levels and $B(E2)$ values were calculated within the shell-model space of the $2p_{1/2}$ and $1g_{9/2}$ orbitals for protons and the $2d_{5/2}$ and $3s_{1/2}$ orbitals for neutrons. The effective interaction between the protons was taken from the work of Gloeckner and Serduke;[14] the "seniority" interaction given in Table II of Ref. 14 was used. The effective proton-neutron (pn) interaction was taken from the work of Gloeckner.[15] Calculations have been made with two sets of pn matrix elements given in Ref. 15. These are labeled "final fit" and "$N=51$ free fit" in Table II of Ref. 15. The "final fit" was obtained from a fit to energy levels of the Zr and Nb isotopes in addition to the energy levels of the $N=51$ nuclei, whereas the "$N=51$ free fit" included the energy levels of the $N=51$ nuclei only.

The energy levels of ^{95}Ru obtained with these interactions are compared with experiment in Fig. 6. As could be expected, the "$N=51$ free fit" interaction gives better agreement with experiment than the "final fit" interaction. The $\frac{7}{2}^+$ level is experimentally lower than calculat-

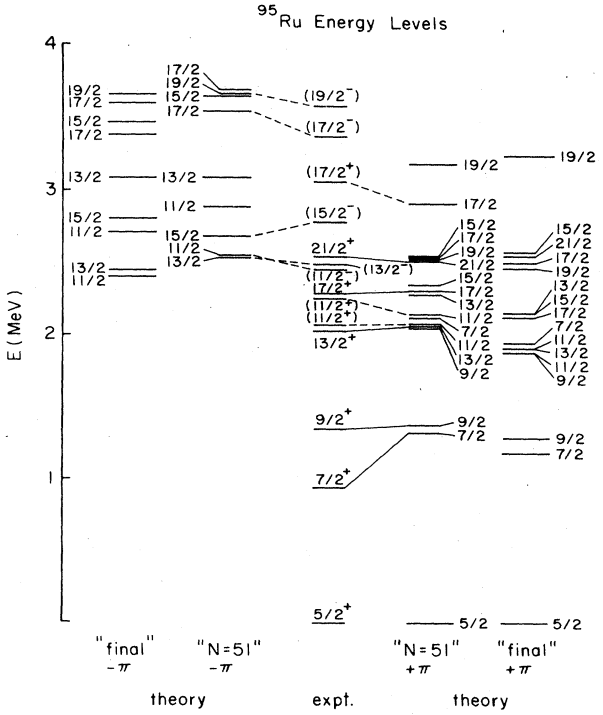

FIG. 6. Energy levels for ^{95}Ru. The experimental levels are shown in the center, with the negative parity theoretical levels on the left and the positive parity theoretical levels on the right, obtained with the "$N=51$ free fit" interaction. Energy levels obtained with the "final fit" interaction are shown on the outside. For the theory, only the lowest two states for each spin and parity are shown. Solid lines connect the calculated levels with the corresponding experimental levels, while dashed lines suggest a possible correspondence.

TABLE III. Comparisons of experimental and theoretical $E2$ matrix elements.

			Interaction				$[B(E2)J_i \rightarrow J_f]$		
			$N=51$ free fit		Final fit		Theory		Expt.
Nucleus	J_i	J_f	A[a]	B	A	B	$N=51$ free fit	Final fit	
^{90}Zr	8	6	4.07	0			66.3		60.5±2.5[b]
	6	4	6.43	0			165.4		
^{91}Zr	$\frac{21}{1}$	$\frac{17}{2}$	3.85	2.28	3.67	3.58	100	119	111±6[c]
	$\frac{17}{2}$	$\frac{13}{2}$	5.74	2.81	5.01	4.61	204	214	
^{92}Mo	8	6	3.49	0			48.7		32.4±1.2[b]
	6	4	5.52	0			121.9		78.5±2.5[b]
^{93}Mo	$\frac{21}{2}$	$\frac{17}{2}$	3.41	1.84	3.46	2.34	75	86	
	$\frac{17}{2}$	$\frac{13}{2}$	5.14	2.43	4.87	3.52	162	176	108±6[c]
^{94}Ru	8	6	0.87	0			3.0		0.094±0.006[b]
	6	4	1.37	0			7.5		2.6±0.2[b]
^{95}Ru	$\frac{21}{2}$	$\frac{17}{2}$	3.55	1.33	3.49	0.62	71.1	57.8	49.5±0.8[d]
	$\frac{17}{2}$	$\frac{13}{2}$	3.58	0.94	3.73	1.07	65.6	72.8	163±15[d]

[a] $[B(E2)J_i \rightarrow J_f]^{1/2} = Ae_p + Be_n$, where e_p and e_n are the proton and neutron effective charges, respectively. The $B(E2)$ values have been calculated using $e_p=2$ and $e_n=1$ (see the text). For the radial matrix elements, harmonic oscillator wave functions with $\hbar\omega=8.78$ MeV were used

[b] See Table IV of Ref. 16.

[c] See Table VI of Ref. 16.

[d] This experiment.

ed, probably due to contamination with the $g_{7/2}$ state which lies outside the model space of the present calculation.

The $B(E2)$ values deduced from the lifetimes of the $\frac{21}{2}^+$ and $\frac{17}{2}^+$ level in ^{95}Ru, together with the $B(E2)$ values for transitions between other high-spin states in this mass region,[16] are given in Table III. Since the wave functions for the high-spin states in ^{90}Z and ^{91}Zr are particularly simple, the experimental strengths for the $8^+ \rightarrow 6^+$ and $\frac{21}{2}^+ \rightarrow \frac{17}{2}^+$ transitions in these two nuclei have been used to fix the "effective charges" at the values of $e_p = 2$ and $e_n = 1$ (see also Ref. 16). The other $B(E2)$ values were then calculated with these fixed effective charges. Comparisons between theoretical and experimental $B(E2)$ values in the *sd* shell, where the model space is completely within a major shell and the effective interaction is relatively well determined, have shown[17] that the effective charge is empirically state and nucleus independent under these circumstances. Thus, the disagreement between experiment and the $B(E2)$ values calculated with constant effective charges is interpreted as an indication of a failure of the model space or interaction.

No evidence of any collective effects was observed in the level scheme of ^{95}Ru. This will be discussed together with the ^{97}Ru results at the end of this section.

B. ^{97}Ru

The strongest γ rays in the decay scheme of ^{97}Ru involve the even parity yrast sequence, and have been drawn to the left of the level scheme in Fig. 5. No shell-model calculations for ^{97}Ru are available for direct comparison with experiment. However, the level structure is very similar to that of $^{95}Mo_{53}$, which has been found to compare favorably with calculations.[3] The even parity levels of ^{97}Ru are compared with those of ^{95}Mo in Fig. 7, where the calculated levels of ^{95}Mo for the $(\pi g_{9/2})^2(\nu d_{5/2})^3$ configuration are also included. The comparison between experimental and theoretical levels in ^{95}Mo and experimental levels in ^{97}Ru have been discussed in some detail in Ref. 3. The $\frac{13}{2}^+$ levels at 1652 and 1826 keV were not observed by them in their (α,xn) studies, and it is not clear from the decay scheme which one of these belongs to the above configuration. Of the four highest spin states of even parity at 3621, 3671, 4264, and 4731 keV, with spins of $\frac{23}{2}^+$, $(\frac{25}{2}^+)$, $(\frac{27}{2}^+)$, and $(\frac{29}{2}^+)$, respectively, the $\frac{23}{2}^+$ and $(\frac{25}{2}^+)$ levels compare well with the calculations for the $(\pi g_{9/2})^2(\nu d_{5/2})^3$ configuration in ^{95}Mo. The $(\frac{27}{2}^+)$ and $(\frac{29}{2}^+)$ levels do not belong to this configuration, which can only couple to a maximum spin of $\frac{25}{2}^+$. A probable configuration for these states is $(\pi g_{9/2})^2(\nu d_{5/2})^2(\nu g_{7/2})$, which can couple to a maximum spin of $\frac{31}{2}^+$.

Similar comparisons between the level schemes of ^{95}Mo and ^{97}Ru have been made by Bucurescu *et al.*,[10] where they include the information of their lifetime measurements. However, changes in the level scheme would necessitate a reanalysis of the state lifetimes for some of the lower-lying levels.

Collective effects were observed in ^{97}Ru in the form of

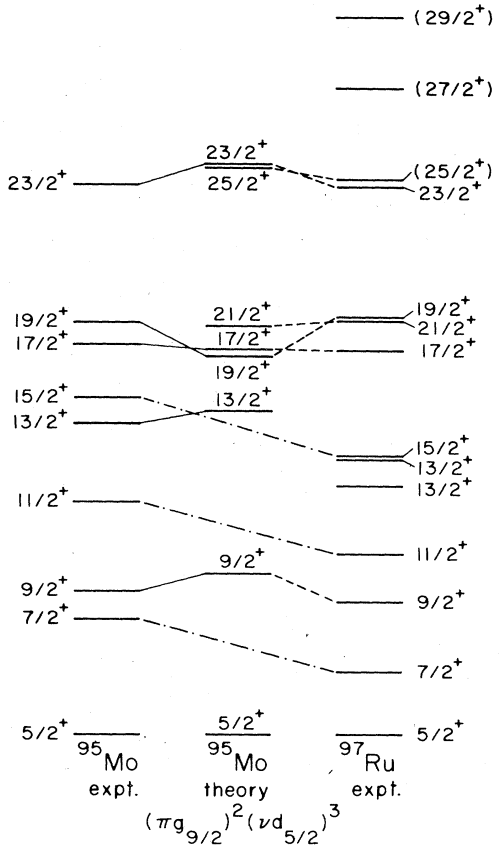

FIG. 7. Even-parity energy levels of ^{97}Ru (from the present work) compared with experimental and calculated energy levels of ^{95}Mo (from Ref. 3). Calculated levels in ^{95}Mo are connected with solid lines to corresponding experimental levels in ^{95}Mo, and with dashed lines to experimental lines in ^{97}Ru, suggesting similar configurations. Dot-dashed lines connect experimentally observed levels in ^{95}Mo and ^{97}Ru expected to have similar structure.

a weak $\Delta J = 2$ band built on an $\frac{11}{2}^-$ state. The systematics of $\Delta J = 2$ bands built on $\frac{11}{2}^-$ states in odd-A $^{97-103}$Ru isotopes are shown in Fig. 8, along with the ground state bands of the neighboring even-even Ru nuclei. These $\Delta J = 2$ bands, which are signatures of modest collectivity, have been described as "decoupled" bands built on the $1h_{11/2}$ quasineutron state, where the $\Delta J = 2$ band spacings follow the ground-state band spacings of the neighboring even-even core nuclei. These spacings increase as N approaches the closed shell of 50, implying less collectivity.

The population strength of the $1h_{11/2}$ quasineutron band is observed to decrease as the $N = 50$ shell closure is approached. The band is considerably weaker in ^{97}Ru ($N = 53$) compared to the ^{99}Ru ($N = 55$) nucleus, and is not observed at all in the ^{95}Ru ($N = 51$) nucleus. The reason for this and for not observing the $h_{11/2}$ band in ^{95}Ru is shown in Fig. 9, where the excitation energies of the $\frac{11}{2}^-$ states are plotted as a function of the neutron number N. The curve rises steeply as N approaches 50, implying that the $\frac{11}{2}^-$ bands become non-yrast, thus making it more difficult to populate by heavy-ion fusion-

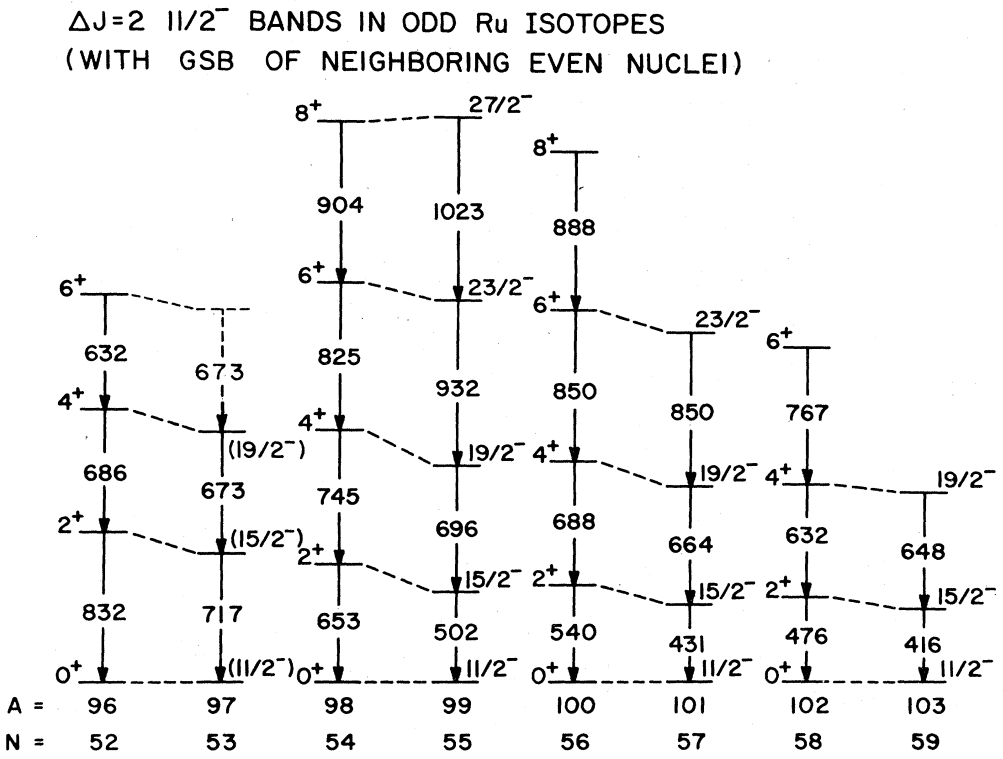

FIG. 8. Systematics of $\Delta J=2$ bands built on $\frac{11}{2}^-$ states in odd-A Ru nuclei, along with the ground state bands (GSB) of the neighboring even-even core nuclei. The γ-ray energies are in keV.

evaporation reactions. A decrease in collective strength as the nuclei tend to a more spherical shape at the $N=50$ shell closure can also contribute to a weakening of the γ-ray cascade.

No evidence for a $\Delta J=1$ band structure built on a $g_{9/2}$ neutron-hole intruder state was found in either of the ^{95,97}Ru nuclei. This suggests that there are significant differences in the environments of the $Z>50$ and $N>50$ regions, leading to different collective properties, especially since the $\frac{9}{2}^+$ $\Delta J=1$ band is such a ubiquitous feature in the $Z>50$ nuclei. Different average potentials are

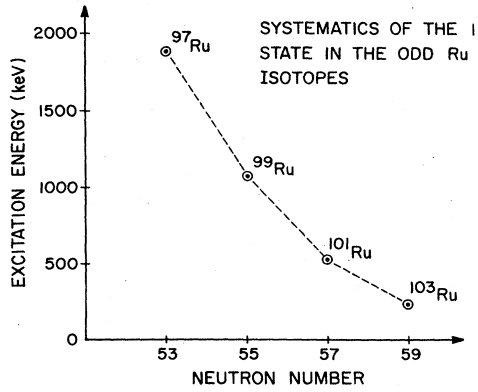

FIG. 9. The $\frac{11}{2}^-$ bandhead energies for odd-A Ru nuclei plotted as a function of the neutron number N.

experienced by the $g_{9/2}$ neutron hole as compared to the $g_{9/2}$ proton hole. There are ~ 16 valence neutrons in the $50<N<82$ shell available for the proton-hole interaction in the $Z>50$ region compared to ~ 6 valence protons in the $38<Z<50$ shell for the neutron hole in the $N>50$ region. The nearer the shell closures, the greater the stability against deformation, in general. The interaction of the $g_{9/2}$ proton hole with the available neutrons leads to a broader potential energy surface in the Sb ($Z=51$) and $I(Z=53)$ nuclei, compared to their neutron analogs, the ^{95}Ru ($N=51$) and ^{97}Ru ($N=53$) nuclei, where the $g_{9/2}$ neutron hole interacts with a fewer number of protons. A broad potential energy surface of the core, indicative of a "softness" towards deformations, is essential in achieving stable potential minima at significant deformations.[18]

V. CONCLUSIONS

The level structures of the ^{95,97}Ru nuclei, with neutron numbers just outside the $N=50$ shell closure, were studied in the present work to probe both shell-model and collective behavior in the $N>50$ region. No collective features were observed in $^{95}Ru_{51}$, and the energy levels were found to be in fair agreement with those calculated within a limited shell-model space. Although no shell-model calculations exist for $^{97}Ru_{53}$, the level structure of ^{97}Ru is found to be dominated by states which can be reasonably well described within the framework of the shell model, by comparison to the experimental and

theoretical energy levels of $^{95}Mo_{53}$. A weak $\Delta J=2$ collective band, built on a $1h_{11/2}$ quasineutron state, was observed in ^{97}Ru. The gradual increase of the band spacings of these $\Delta J=2$ bands in the odd-A Ru nuclei as the $N=50$ shell closure is approached is interpreted primarily as a decrease in collectivity as the nuclei tend toward a spherical shape. No $\Delta J=1$ band structure built on $1g_{9/2}$ neutron holes (analogous to $1g_{9/2}$ proton hole $\Delta J=1$ structures in $Z>50$ nuclei) was observed in the ^{95,97}Ru nuclei. Thus the collective phenomena in the $N>50$ region seem to be quite different from the $Z>50$ region, probably because significantly different average potential energy surfaces exist in the two cases.

It is hoped that these results, which provide information on the sensitive $N>50$ region where there is a gradual transition from spherical shell-model behavior to collective phenomena, will serve both as motivation and as stringent test cases for more comprehensive theoretical calculations.

This work was supported in part by the National Science Foundation.

---

*Present address: Materials Science Laboratory, Reactor Research Centre, Kalpakkam 603102, India.

†Present address: Michigan State University, East Lansing, MI 48824.

‡Present address: Physics Department, University of Notre Dame, Notre Dame, IN 46556.

§Present address: California Institute of Technology, Pasadena, CA 91125.

**Present Address: Oak Ridge National Laboratory, Oak Ridge, TN 37830.

[1]J. B. Ball, J. B. McGrory, and J. S. Larsen, Phys. Lett. **41B**, 581 (1972).

[2]J. B. Ball, J. B. McGrory, R. L. Auble, and K. H. Bhatt, Phys. Lett. **29B**, 182 (1969).

[3]C. M. Lederer, J. M. Jaklevic, and J. M. Hollander, Nucl. Phys. **A169**, 489 (1971).

[4]A. K. Gaigalas, R. E. Shroy, G. Schatz, and D. B. Fossan, Phys. Rev. Lett. **35**, 555 (1975); R. E. Shroy, A. K. Gaigalas, G. Schatz, and D. B. Fossan, Phys. Rev. C **19** 1324 (1979); W. F. Piel, Jr., U. Garg, M. A. Quader, P. M. Stwertka, S. Vajda, and D. B. Fossan, *ibid.* **31**, 456 (1985).

[5]D. M. Gordon, M. Gai, A. K. Gaigalas, R. E. Shroy, and D. B. Fossan, Phys. Lett. **67B**, 161 (1977); D. B. Fossan, M. Gai, A. K. Gaigalas, D. M. Gordon, R. E. Shroy, K. Heyde, N. Waroquier, H. Vincx, and P. van Isacker, Phys. Rev. C **15**, 1732 (1977).

[6]R. E. Shroy, D. M. Gordon, M. Gai, D. B. Fossan, and A. K. Gaigalas, Phys. Rev. C **26**, 1089 (1982); M. Gai, D. M. Gordon, R. E. Shroy, D. B. Fossan, and A. K. Gaigalas, *ibid.* **26**, 1101 (1982).

[7]U. Garg, T. P. Sjoreen, and D. B. Fossan, Phys. Rev. C **19**, 217 (1979).

[8]R. D. McKeown, R. E. Shroy, T. P. Sjoreen, B. A. Brown, and D. B. Fossan, Bull. Am. Phys. Soc. **20**, 719 (1975).

[9]P. Chowdhury, A. Neskakis, U. Garg, T. P. Sjoreen, and D. B. Fossan, Bull. Am. Phys. Soc. **22**, 1028 (1977).

[10]D. Bucurescu, G. Constantinescu, M. Ivascu, W. Andretscheff, B. Bochev, and T. Kutsarova, J. Phys. G **6**, 103 (1980).

[11]H. E. Hseuh, E. C. Macias, D. G. Sarantities, M. Brenner, and W. Klamra (unpublished).

[12]C. L. Hollas, K. A. Aniol, D. W. Gebbi, M. Borsaru, J. Nurzyuski, and L. O. Barbopoulous, Nucl. Phys. **A276**, 1 (1977).

[13]L. R. Medsker and L. H. Fry, Jr., Phys. Rev. C **15**, 649 (1977).

[14]D. H. Gloeckner and F. J. D. Serduke, Nucl. Phys. **A220**, 477 (1974).

[15]D. H. Gloeckner, Nucl. Phys. **A253**, 301 (1975).

[16]B. A. Brown, P. M. S. Lesser, and D. B. Fossan, Phys. Rev. C **13**, 1900 (1976).

[17]B. A. Brown, B. H. Wildenthal, W. Chung, S. E. Massen, M. Bernas, A. M. Berstein, R. Miskimen, V. R. Brown, and V. A. Madsen, Phys. Rev. C **26**, 2247 (1982).

[18]K. Heyde, P. van Isacker, M. Waroquier, J. L. Wood, and R. A. Meyer, Phys. Rep. **102**, 291 (1983).